BioNanoScience (2023) 13:339–351
https://doi.org/10.1007/s12668-023-01093-2

RESEARCH

Eugenol Loaded Ag-Ti-Co Nanocomposite as a Promising Antimicrobial and Antioxidative Agent

Aarya Sahay[1] · Rajesh Singh Tomar[1] · Vikas Shrivastava[1] · Pallavi Singh Chauhan[1]

Accepted: 28 March 2023 / Published online: 5 April 2023

Abstract

The present study aims to synthesize and characterize eugenol-loaded nanocomposite (using *Syzygium aromaticum*), followed by drug loading and analysis of drug release kinetics using standard procedure. UV–Vis spectroscopy showed absorption band at 258 nm, FTIR revealed the availability of eugenol, and SEM analysis and X-ray diffractometer examination revealed average particle diameter of 42.67 nm with orthorhombic structure. Energy dispersive X-ray (EDAX), Zeta, and size distribution pattern also confirmed the elemental composition, formation of stable nanocomposite, and uniformity of synthesized nanocomposite, respectively. MIC value obtained for *Escherichia coli*, *Staphylococcus aureus*, and *Pseudomonas aeruginosa* was 6.25 µg/ml, and for *Proteus mirabilis*, it is 3.25 µg/ml. MBC value for *Escherichia coli* and *Proteus mirabilis* was 12.5 µg/ml, and for *Staphylococcus aureus* and *Pseudomonas aeruginosa*, it was 25 µg/ml. Antioxidant studies revealed that Eu@NC showed significant DPPH free radical scavenging activity. This biosynthesized Eu@NC with enhanced antibacterial activity could be less toxic to environment and an eco-friendly approach.

Keywords Eugenol · Nanocomposite · Nanoparticle characterization · Antimicrobial activity · Antioxidant activity · Drug loading · Drug release kinetics

1 Background

Nanotechnology has resulted in various scientific advancements, which functions as a fundamental unit [1]. Many agencies such as proteins, medicines, dendrites, DNA, RNA [2], and ligand improve nanoparticle application in delivery of drugs [3, 4] for the treatment of many conditions such as wound infection, gene therapy, malignancies, and many more [5, 6]. The cobalt, titanium, and silver nanoparticles have emerged as promising tool in drug delivery [7, 8]. Factors such as desiccation, infection [9], maceration, necrosis, pressure, trauma, and edema [10] can all impede wound healing [11]. *Syzygium aromaticum* (cloves) are aromatic flower buds [12] that belong to *Myrtaceae* family [13]. It has been known to be a rich source of phenolic chemicals including eugenol, eugenol acetate, and gallic acid [14]. Eugenol extracted from clove buds has been reported to contain different phytochemicals like flavones, aldehyde, and phenol.

The aggrandized prospects of nanoparticles in different biomedical application have led to the quest of their synthesis using different methodology like chemical, physical, and biological [15]. However, the biological method has been mostly recognized in this decade due to their eco-friendly preparation method and the use of non-hazardous chemicals. These methodologies have been called as green methods of synthesis [16]. Green synthesis of the nanoparticle is mainly used due to its advantages like eco-friendly approach, easily availability of the biological materials, and rapid process [17–19].

The biosynthesis of nanoparticles by plant extract gives an advancement over other green methods as it is simple, environment friendly, cost-effective, and relatively reproducible [20]. Plant extracts have the potential to act as both reducing agent and stabilizing agent in the nanoparticle synthesis [13, 14], and it affects the features of the synthesized nanoparticles also [21, 22]. The synthesis has been successfully reported to form nanoparticles

✉ Rajesh Singh Tomar
rstomar@amity.edu

[1] Amity Institute of Biotechnology, Amity University Madhya Pradesh, Gwalior 474005, India

because of the presence of several concentrations and amalgamations of organic reducing agents in variety of plant extracts [23, 24]. The various phases included in the process of nanoparticle synthesis involve the activation phase, which includes metal ion reduction, and then their nucleation [25]. The primary phase is nanoparticle synthesis using plant extracts, the second phase (growth phase) is tiny nanoparticles and coalesce, and the final phase is the termination phase, during which the nanoparticles take on their final shape [26].

Evaluation of drug release is crucial in the biomedical field, as it is important for the analysis of drug release type [19]. The importance of kinetic models is often helpful in elucidating release mechanisms and that can be of use in the control of release mechanism [20, 27]. Further advantage of the kinetics is to signify various release data with one or two parameters. Results obtained from such a different standard model can be employed for evaluating different delivery systems of a drug [28]. Drug release studies have a fundamental role in analyzing the release of drug in different dosage [29]. A theoretical justification of the best models is evaluated by different mathematical models [22, 23].

The aim of the study is to determine the antimicrobial activity of eugenol-loaded nanocomposite against wound-associated pathogens, evaluation of minimum inhibitory concentration (MIC), and minimum bactericidal concentration test (MBC). This study is of the opinion that eugenol-loaded nanocomposite with significant antimicrobial activity may enhance the wound healing with special reference to impaired wound healing in diabetes.

2 Materials and Methods

2.1 Materials

Silver nitrate ($AgNO_3$), cobalt nitrate ($CoNO_3$), and titanium dioxide (TiO_2) were purchased from Merck. Polyvinylpyrrolidone (PVP), 1,1-diphenyl-2-picrylhydrazyl (DPPH), and other components were purchased from Sigma-Aldrich.

2.2 *Syzygium aromaticum* Extract Preparation

Dried clove buds were collected and powdered using mortar and pestle, and 1 gm of the powder was dissolved in 100 ml of a 40% butanol solution and continuously shaken in a rotary shaker for 3–4 h. The extract was then filtered through Whatman filter paper, and a crude extract was prepared [30].

2.3 Nanocomposite Synthesis and Characterization

The synthesis of Ag-Ti-Co NC was done was done by using eugenol extracts obtained from *Syzygium aromaticum (S. aromaticum)*. Plant extract was added dropwise into a solution containing $AgNO_3$ (0.001 M) contained with Titanium dioxide (TiO_2) (0.001 M) and Cobalt Nitrate ($CoNO_3$) (0.01 M) stirred at 350 rpm for 2 h at 60 °C [31]. PVP (polyvinyl pyrrolidone) (0.001 mM; 0.5 ml) was added into the solution. The formation of color change indicated the synthesis of nanocomposite. The synthesized Ag-Ti-Co nanocomposite was characterized by UV–Vis spectroscopy, X-ray diffraction (XRD) powder method, Fourier transform infrared (FTIR) spectroscopy, Energy dispersive X-ray (EDAX), ZETA Sizer and scanning electron microscope (SEM) (Model JSM6100) analysis. Different parameters of the nanocomposite such as shape, nature, size of the particles, crystallinity, surface area, charge and stability are obtained by these techniques [32].

2.4 Loading of Eugenol on Nanocomposite

The loading of eugenol on prepared nanocomposite was done through sonication technique. Five hundred microgram/milliliter of nanocomposite was dissolved in eugenol and bath sonicated for 15 min [33]. Allowed to be kept on dissolved in distilled water through a sonicator and in a different vial, 500 µg/ml of eugenol was prepared. Then, the sample was centrifuged at 8000 rpm for 10 min and filtered through a cellulosic white membrane filter. Followed by the filtration, the supernatant was collected to determine the loading amount of eugenol [28]. The loading capacity was calculated based on the following formula:

$$\%\text{Eugenol loading} = \frac{\text{Amount of eugenol added initially} - \text{amount of eugenol in supernatant}}{\text{Amount of eugenol added initially}} \times 100$$

The eugenol-loaded nanocomposite (Eu@NC) (collected on the pellet was dried under 30–40 °C and washed with 40% ethanol [34].

2.5 Drug Release Kinetics

Drug release of eugenol-loaded nanocomposite was analyzed separately by two methods given with some modification, i.e., direct method and dialysis bag method [28, 35].

2.5.1 Direct Addition Method

Five hundred microgram of eugenol-loaded nanocomposite (Eu@NC) was added in a tube containing 2 ml of buffer with pH 7 and shaked continuously. A small aliquot of dissolution fluid was withdrawn at different time intervals and maintained with an equal volume of the buffer after per withdrawal. The collected samples were centrifuged for 10 min at 10,000 rpm, and supernatant was analyzed by UV–visible spectrophotometer at 543 nm [36].

2.5.2 Dialysis Method

Eu@NC was dialyzed against 40-ml buffer (pH 7) at 25 °C with constant stirring at 100 rpm. At different time intervals, sample was pipetted out (2 ml) and was analyzed spectrophotometrically. Simultaneously, add an equal amount of buffer (2 ml) during every cycle of sample collection [35].

Different types of mathematical models are used for evaluating drug dissolution [28] to determine the mechanism of drug release.

Zero-order equation:

$$Q_t = Q_0 + K_0^t$$

Here, Q_t is the quantity of drug dissolved in time t, K_0 is the zero-order release (concentration/time) constant, and Q_0 is the initial quantity of drug in the solution, mostly $Q_0 = 0$.

First-order equation:

$$\log C = \log C_0 - K_t/2.303$$

Here, C_0 is the initial concentration of drug and K is the first-order constant.

Higuchi's equation:

$$Q_t = K_H t^1_{/2}$$

Here, K_H is the release rate constant (Higuchi model) and Q_t is the amount of drug released in time t.

$$Mt/M\overline{\alpha} = Kt^n$$

where $Mt/M\,\bar{\alpha}$ is a fraction of drug released at time t. K is the release rate of constant, and n is the release exponent.

2.6 Evaluation of Antimicrobial Activity

Antimicrobial activity of Eu@NC (Eu @Ag-Ti-Co NC) was estimated using well diffusion method against four wound-associated microorganisms *E. coli* (MTCC-40), *Proteus mirabilis* (MTCC-3310), *Pseudomonas aeruginosa* (MTCC-424), and *Staphylococcus aureus* (MTCC-9760). 0.5 McFarland standard (10^8 CFU per ml) was used for estimation of antimicrobial activity.

2.7 Minimum Inhibitory Concentration (MIC) and Minimum Bactericidal Concentration (MBC)

MIC of Eu@NC for *Escherichia coli* (MTCC-40), *Proteus mirabilis* (MTCC-3310), *Pseudomonas aeruginosa* (MTCC-424), and *Staphylococcus aureus* (MTCC-9760). The Minimum inhibitory concentration value of loaded nanocomposite conjugate and others was estimated according to the standard method [37]. All experiments were conducted in triplicate. Five hundred microgram/milliliter stock solution was prepared, and two-fold serial dilutions of the eugenol-loaded nanocomposite were carried out. 96-well microtiter plate was used for the MIC test by standard broth microdilution processes [38]. After 24 h, measurements were taken using ELISA reader. The lowest concentration of nanocomposites that inhibits the growth of bacteria was taken as a MIC [39]. MBC analysis was performed by plating the suspension [40]. The lowest concentration that shows no visible growths is taken as the MBC value [41].

2.8 Antioxidant Activity

The Eu@NC DPPH assay [42] was assessed for eugenol, eugenol-loaded nanocomposite, and unloaded nanocomposite using the standard technique [43]. The obtained solution was kept in the dark for 30 min and measured at 517 nm using by UV–vis spectrophotometer. The percentage of scavenging activity was calculated as follows:

$$\text{DPPH free radical scavenging (\%)} = \frac{\text{control} - \text{sample}}{\text{control}} \times 100$$

3 Results and Discussion

3.1 Nanocomposite Synthesis and Their Characterization

In nanoparticle synthesis, there are three fundamental phases of metal nanoparticle synthesis with plant extracts [44]: firstly, the activation phase in which metal ions are reduced and metal atoms are formed; during the second phase, which is the growth phase, the small nanoparticles spontaneously coalesce into large particle size; and the third phase called termination phase gives the final shape of the nanoparticles [45]. The synthesis of Eu@NC is achieved by reducing silver nitrate, titanium dioxide, and cobalt nitrate (0.001 M, 0.001 M, 0.01 M, respectively), with eugenol as a reducing agent and PVP as a capping agent. The changes in the color of the solution after the addition of plant extract, from pink to deep brown precipitate, confirmed the formation of the nanocomposite. The color change of the precipitate can be reasoned to the shift of the surface plasmon band because of the size changes of the particle [46, 47].

Further, the biosynthesized Eu@NC was characterized by FTIR spectroscopy, SEM, XRD, EDAX, ZETA, size distribution pattern, and UV–Vis spectroscopy to determine their physiochemical properties.

3.1.1 UV–Vis Spectroscopy Analysis

Surface plasmon resonance (SPR), also known as surface plasmon excitation, is a phenomenon that arises when applied electromagnetic fields excite surface plasmons on the surfaces of nanoparticles [36, 37]. Sarekha et al. previously discussed that eugenol-loaded nanoparticle range comes between 250 and 300 nm range. The UV–visible absorbance spectrum of the synthesized Eu@NC displayed a broad peak at 258 nm. The absorption peak can be attributed to the surface plasmon resonance of tri-metallic nanocomposite [48]. The data indicated the loading of eugenol into tri-metallic nanocomposite.

3.1.2 FTIR Spectroscopy

FTIR is a technique for the characterization of nanoparticles that can be used for the analysis of the vibration frequencies of bonds present between the molecules [38, 40]. FTIR analysis determined the phytochemicals likely to be responsible for the reduction and capping of reduced silver, titanium, and cobalt nanoparticles with surface adsorbent characteristics.

As shown in Fig. 1, the FTIR results of eugenol gave characteristic peak at 3551 cm^{-1}, 3476 cm^{-1}, 3413 cm^{-1}, 3236 cm^{-1}, 2929 cm^{-1}, 2030 cm^{-1}, 1637 cm^{-1}, 1617 cm^{-1}, 1381 cm^{-1}, 1362 cm^{-1}, 1204 cm^{-1}, 1043 cm^{-1}, 620 cm^{-1}, 480 cm^{-1}, and 408 cm^{-1} which corresponds to O–H stretch vibration of phenol, O–H stretch vibration of carboxylic acid, N–H stretch vibration of amines, C-H stretch vibration of alkane, C-H stretch vibration of alkanes, C≡C stretch vibration of alkyne, C–C stretch vibration of aromatic ring, C–C stretch vibration of allyl group, C-H stretch vibration of alkane, C-H stretch vibration of alkyl methyl, -C–O–C- stretch vibration of alcohol, -CH-CH2 stretch vibration of vinyl group, C-S stretch vibration of halo compound, and C-S stretch vibration of halo compound, respectively [49].

The FTIR spectrum of the Eu@NC is shown in Fig. 1. The biosynthesis of tri-metallic nanocomposite loaded with eugenol gave characteristic peaks. The peaks at

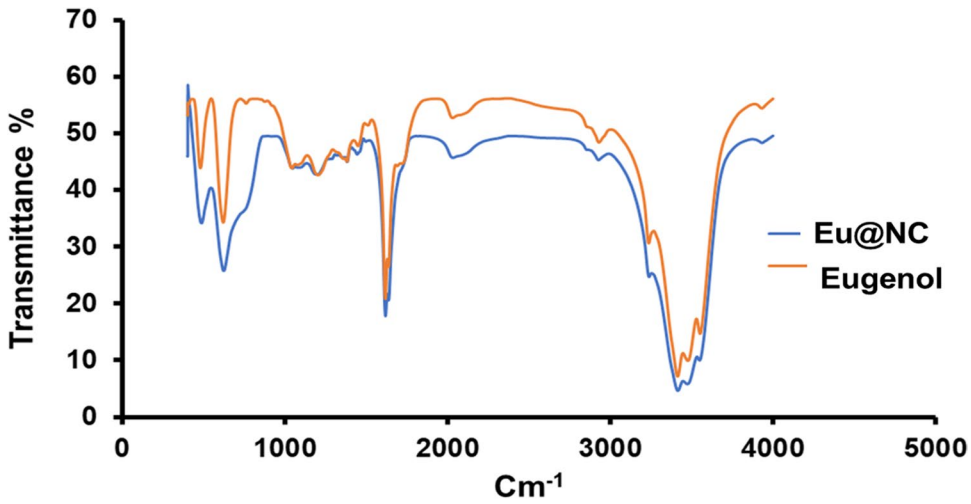

Fig. 1 Physiochemical characterization of nanomaterials determined by FTIR spectra of eugenol and Eu@NC

3551 cm^{-1}, 3476 cm^{-1}, 3413 cm^{-1}, 3236 cm^{-1}, 2929 cm^{-1}, 2030 cm^{-1}, 1637 cm^{-1}, 1618 cm^{-1}, 1497 cm^{-1},1444 cm^{-1}, 1382 cm^{-1}, 1195 cm^{-1}, 1047 cm^{-1}, 1082 cm^{-1}, 23 cm^{-1}, and 488 cm^{-1} were N–H stretch vibration of amines, C-H stretch vibration of alkane, C-H stretch vibration of alkane, C≡C stretch vibration of alkyne C–C stretch vibration of allyl, C–C stretch vibration of allyl, C = O stretch vibration of ketone, C = O stretch vibration of carbonyl group, C-H stretch vibration of alkane, -C–O–C- stretch of alcohol, C–O–C stretch vibration of ether, C–O–C stretch vibration of ether, C-S stretch vibration of halogen compound, respectively. The presence of similar peaks was considered for the presence of eugenol which has been reported previously [49].

3.1.3 XRD Analysis

The XRD spectra were utilized to verify the crystalline nature of the tri-metallic nanocomposite. The XRD spectrum of Eu@NC exhibited strong peaks at 2θ values: 32.1512, 38.079, 46.1373, 47.9564, and 54.7137 corresponding to (111), (200), (211), (220), and (221) planes, respectively (Fig. 2). The different peaks corresponded to the standard peaks of silver, titanium, and cobalt nanocomposite reported in JCPDS 21–1272 and 80–1538. As calculated, the lattice parameter of eugenol-loaded Ag-Ti-Co nanocomposite was found to be 4.6344 Å. The average nanocomposite size is calculated by the Debye Scherrer equation: $D = K\lambda/\beta \cos\theta$ where D is the average particle size, λ (1.5406 ° A); β is the full width at half maximum of the peak (FWHM), k (constant 0.9); and θ is the diffraction angle. The average calculated crystal size of Eu@NC was found as 41 nm, corresponding to orthombic structures [41, 42].

3.1.4 SEM and EDAX Analysis

The surface morphology and size of the Eu@NC were determined and validated by SEM [43, 44] equipped with EDS, and SEM results indicated the size of the nanocomposite in the nanorange (10–100 nm) shown in Fig. 3. The EDS analysis of Eu@NC is shown in Fig. 4. The result demonstrates the clear elemental composition profile of the biosynthesized eugenol-loaded Ag-Ti-Co nanocomposite. The validation of the presence of silver, titanium, and cobalt in synthesized nanocomposite confirmed the formation of a tri-metallic nanocomposite,

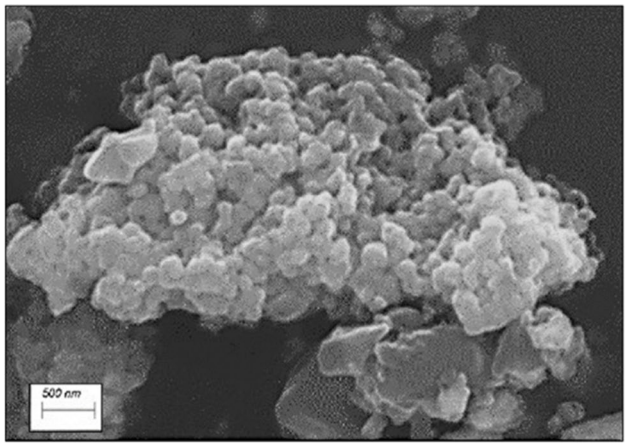

Fig. 3 Physiochemical characterization of nanomaterials determined by SEM image of the Eu@NC

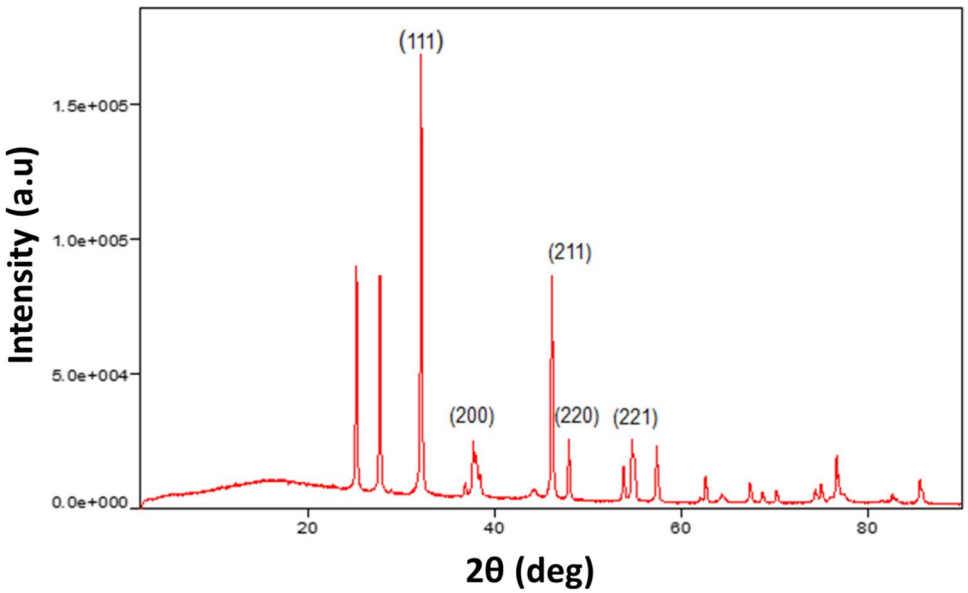

Fig. 2 Physiochemical characterization of nanomaterials determined by XRD spectra of Eu@NC

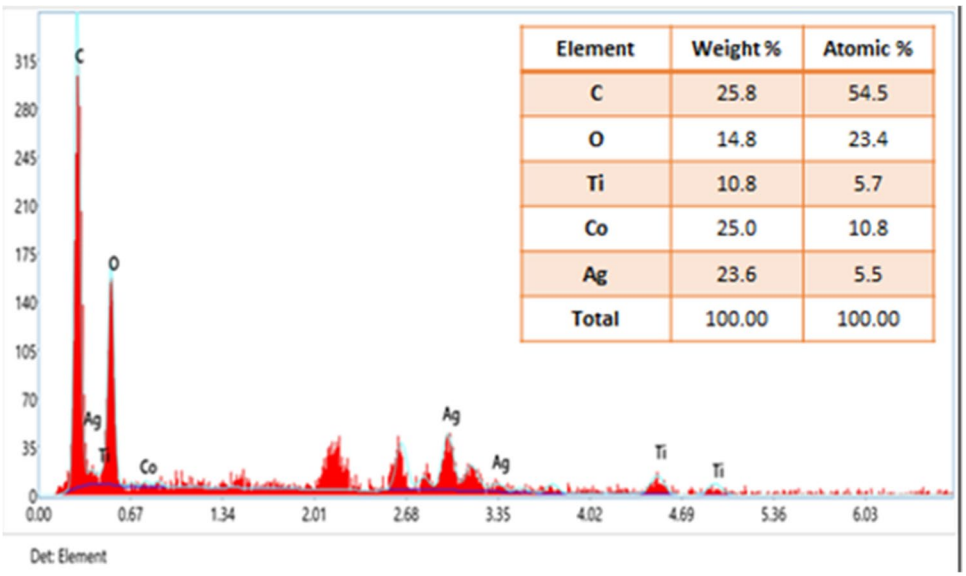

Fig. 4 Physiochemical characterization of nanomaterials determined by EDS analysis of Eu@NC

and the presence of oxygen and carbon was also found which may be due to the loading of eugenol ($C_{10}H_{12}O_2$).

3.1.5 Stability Analysis

The Zeta potential is a characterization technique to measure the magnitude of the electrical charge present on the lipid bilayer, which is used to evaluate the charge stability of a dispersed system [50, 51]. An electric charge is applied over the sample for measuring the Zeta potential of the nanoparticle in a folded capillary flow cell [52]. It is significant to examine the stability of nanocomposite in a medium to consider its complementary effect. Accumulation and stability depend on the charge of the nanoparticles [53].

The Zeta potential of synthesized Eu@NC was found to be − 34.3 mV with PDI value 1.000 (Fig. 5) which indicated the net negative charge at the surface of the synthesized nanoparticles. PDI value is basically a representation of the distribution of size populations within the sample according to the PDI value of the sample that shows the highly polydisperse sample. Zeta potential results confirmed the stability of synthesized EU@NC. Zeta potential's absolute value indicates a high electric charge on the surface of the eugenol-loaded nanocomposite, which has potent repulsive effects between particles to stop the nanocomposite in the solution from aggregating [54].

3.2 Antimicrobial Activity of Eu@NC

3.2.1 Well Diffusion Assay

As shown in Fig. 6, the antimicrobial activity of the Eu@NC showed significant antimicrobial activity against wound-causing pathogens as compared with eugenol, the antimicrobial activity of eugenol-loaded nanocomposite against *E. coli*, *S. aureus*, *P. aeruginosa*, and *Proteus mirabilis* (i.e., 16 mm, 17 mm, 14 mm, and 21 mm, respectively). The antimicrobial activity of this eugenol-loaded Ag-Ti-Co trimetallic nanocomposite is not yet performed in any previous research work. This unique investigation was performed in our research work.

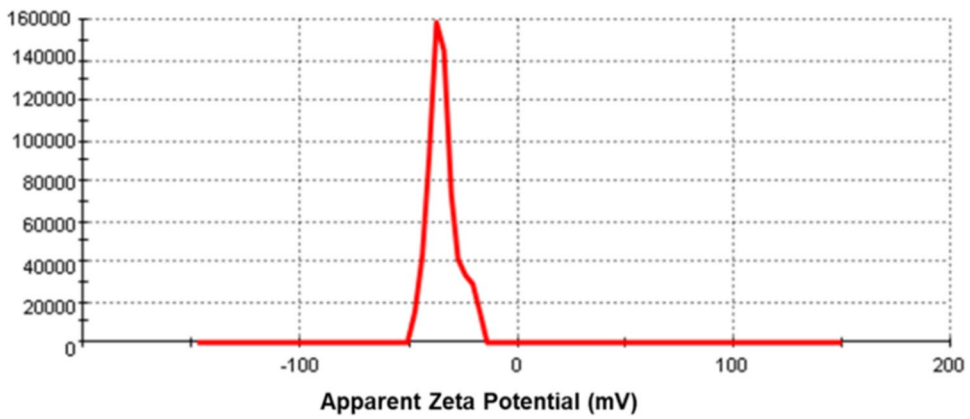

Fig. 5 Physiochemical characterization of nanomaterials determined by Zeta potential analysis of Eu@NC

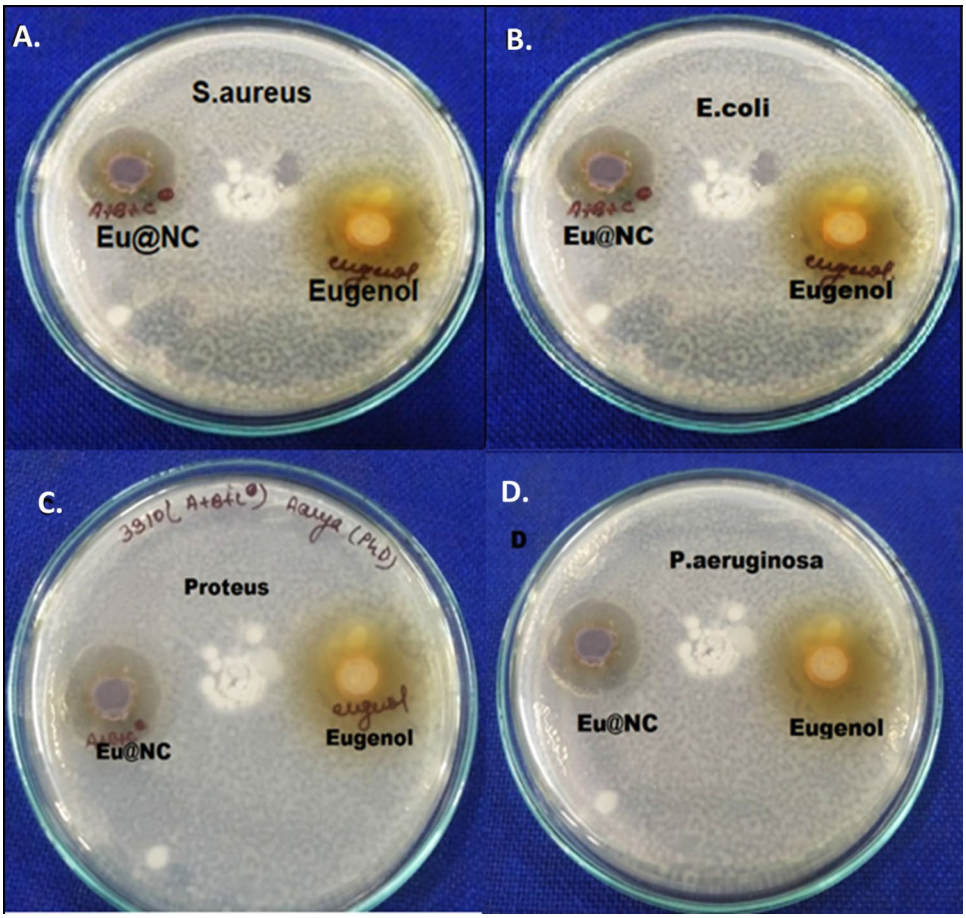

Fig. 6 Antimicrobial activity of of eugenol and eugenol-loaded nanocomposite (Eu@NC) in wound-associated pathogens

3.2.2 MIC and MBC value of Eu@NC

The MIC and MBC value of eugenol-loaded nanocomposite against *E. coli*, *P. aeruginosa*, *Proteus mirabilis*, and *S. aureus*. The MIC (minimum inhibitory concentration) of eugenol-loaded nanocomposite was analyzed in microtiter plate by ELISA reader. The MBC value was observed by the agar plate method. The MIC value of Eu@NC is shown in Table 1, the MBC value is shown in Table 2, and Fig. 7 shows the 96-well microtiter plate. The minimum bacterial concentration of nanocomposite was analyzed in microtiter plate. Wells of the microtiter plate contain nanocomposite ranging from 3.125 to 0.098 µg/ml showed bacterial growth, whereas no growth was seen in wells containing nanocomposite 6.25 to 50 µg/ml. But in the case of *Proteus mirabilis,* no growth observed at 3.125 µg/ml concentration. One hundred microliter of the sample was poured on an agar plate, and after 24 h of incubation, no bacterial growth was observed (Table 2) at particular concentration of nanocomposite. The result determined the MIC and MBC value of the nanocomposite and confirmed its antimicrobial activity. The phenomenon can be reasoned to the three possible ways for the antimicrobial activity of nanocomposite: (a) eugenol-loaded nanocomposite may bind to the bacterial cell wall and degrade the membrane integrity and cell respiratory functions also; (b) eugenol-loaded nanocomposite may penetrate inside the bacterial cell

Table 1 Minimum inhibitory concentration (MIC) value of eugenol-loaded nanocomposite analyzed by ELISA reader against different wound-causing pathogens: (A) *Proteus*, (B) *Staphylococcus aureus*, (C) *P. aeruginosa*, and (D) *E. coli*. Positive (+), indicating growth; Negative (−), indicating absence of growth

Bacteria	50 µg/ml	25 µg/ml	12.5 µg/ml	6.25 µg/ml	3.125 µg/ml	1.5625 µg/ml
E. coli	−	−	−	−	+	+
S. aureus	−	−	−	−	+	+
P. aeruginosa	−	−	−	−	+	+
Proteus	−	−	−	−	−	+

Table 2 Minimum bactericidal concentrations (MBC) of eugenol-loaded nanocomposite after 24 h. *E.coli* (12.5 µg), *S. aureus* (25 µg), *P. aureginosa* (25 µg), and *Proteus* (12.5 µg). Positive (+), indicating growth; Negative (−), indicating no growth

Bacteria	50 µg/ml	25 µg/ml	12.5 µg/ml	6.25 µg/ml
E. coli	−	−	−	+
S. aureus	−	−	+	+
P. aeruginosa	−	−	+	+
Proteus	−	−	−	+

and generate cell death; and (c) nanocomposite may release nanoforms of metal ion which cause bactericidal effect [55].

3.3 DPPH Radical Scavenging Activity

The antimicrobial activity of the nanocomposite was hypothesized to be mediated through the antioxidant property of the nanocomposite [48, 56]. The antioxidant activity was investigated using the radical scavenging (DPPH) experiment. A stable free radical called DPPH reacts with a hydrogen donor. After reacting, the DPPH radical produces the reduced form of DPPH that is hydrazine form, which changes from purple to yellow color. The loss of color is due to the antioxidant content [57]. Eugenol extract shows 86.8% inhibition, eugenol-loaded nanocomposite 67.1% inhibition, and unloaded nanocomposite 36.3% inhibition which could be related to crosslinking. A graph is shown in Fig. 8, and different samples are shown in Fig. 8a. Pure eugenol shows high inhibition compared to other samples, and the loaded nanocomposite shows high inhibition compared to the unloaded nanocomposite.

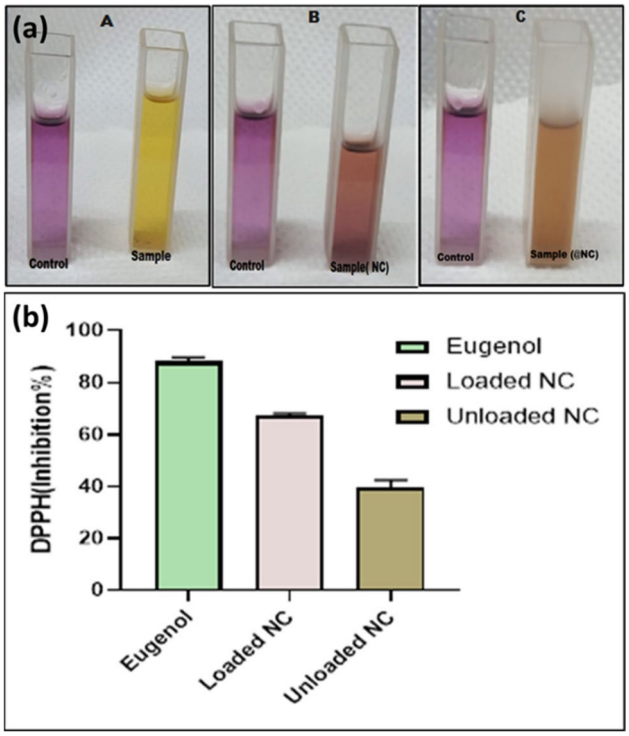

Fig. 8 **a** DPPH-RSA activity of three different samples: (A) eugenol, (B) nanocomposite (NC), and (C) loaded nanocomposite (@NC). **b** DPPH-RSA inhibition percentage for eugenol, loaded nanocomposite, and unloaded nanocomposite

3.4 Drug Release Kinetics

Different kinetic models were used to perform analysis of in vitro drug release (Fig. 9) [49, 58]. Kinetics analysis of the dialysis method and the direct method is shown in Fig. 10

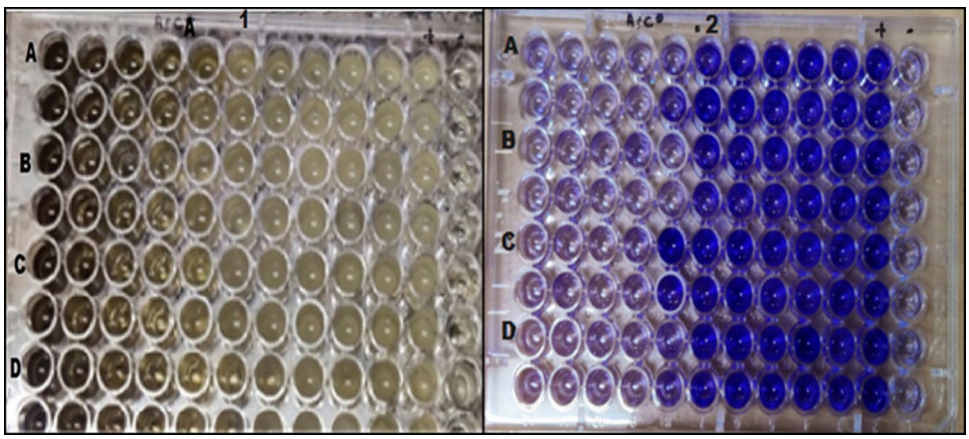

Fig. 7 Pictorial presentation showing 96-well plate set up for the finding of the MIC value of Eu@NC using the broth microdilution method. Nutrient broth media was used in the microdilution assay. Each test well possesses 100 µl of defined Eu@NC dilution and 100 µl of 0.5 McFarland solution of the bacterial suspension. Negative control wells have media only to provide turbidity control. The positive control contained 100 µl of nutrient broth and 100 µl of 0.5 McFarland bacterial culture. **1** 24 h incubation without staining; **2** 24 h incubation with staining. Wells contained different bacterial cultures: (**A**) *E. coli*, (**B**) *Proteus*, (**C**) *P. aeruginosa*, and (**D**) *S. aureus*

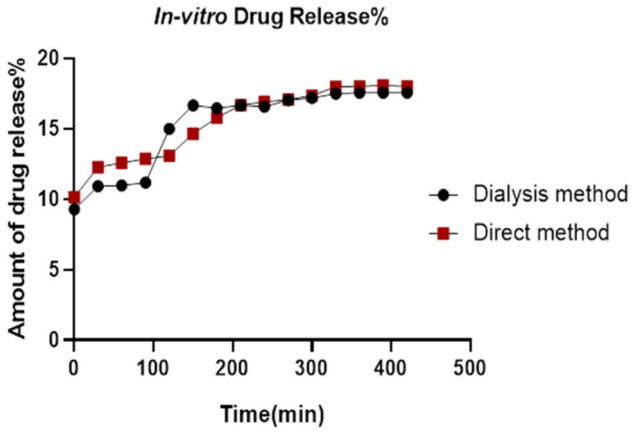

Fig. 9 In vitro eugenol release from nanocomposite at pH 7: direct method and dialysis method

and Fig. 11. The maximum degree of correlation coefficient determined the proper mathematical model that follows release kinetics [59]. In the dialysis method, the results obtained for drug release follow Kosermayer Peppas model, with an R^2 value of 0.9487. As per Kosermayer Peppas model, R^2 value < 0.89 follows non-Fickian release, which describes drug release type, diffusion, and dissolution. In the direct method, drug release data were best fitted with the Higuchi drug release model, with an R^2 value of 0.9511. Higuchi release model describes the diffusion type of drug release (Fig. 11). Thus, in vitro drug release performed by both the methods, direct and dialysis bag method, is approximately equal to the burst release of eugenol from the nanocomposite.

The study showed a novel way to synthesize eugenol loaded tri-metallic nanocomposite (Ag-Ti-Co) using green methodology. Synthesized nanocomposite was well characterized using different techniques. UV–Vis determined

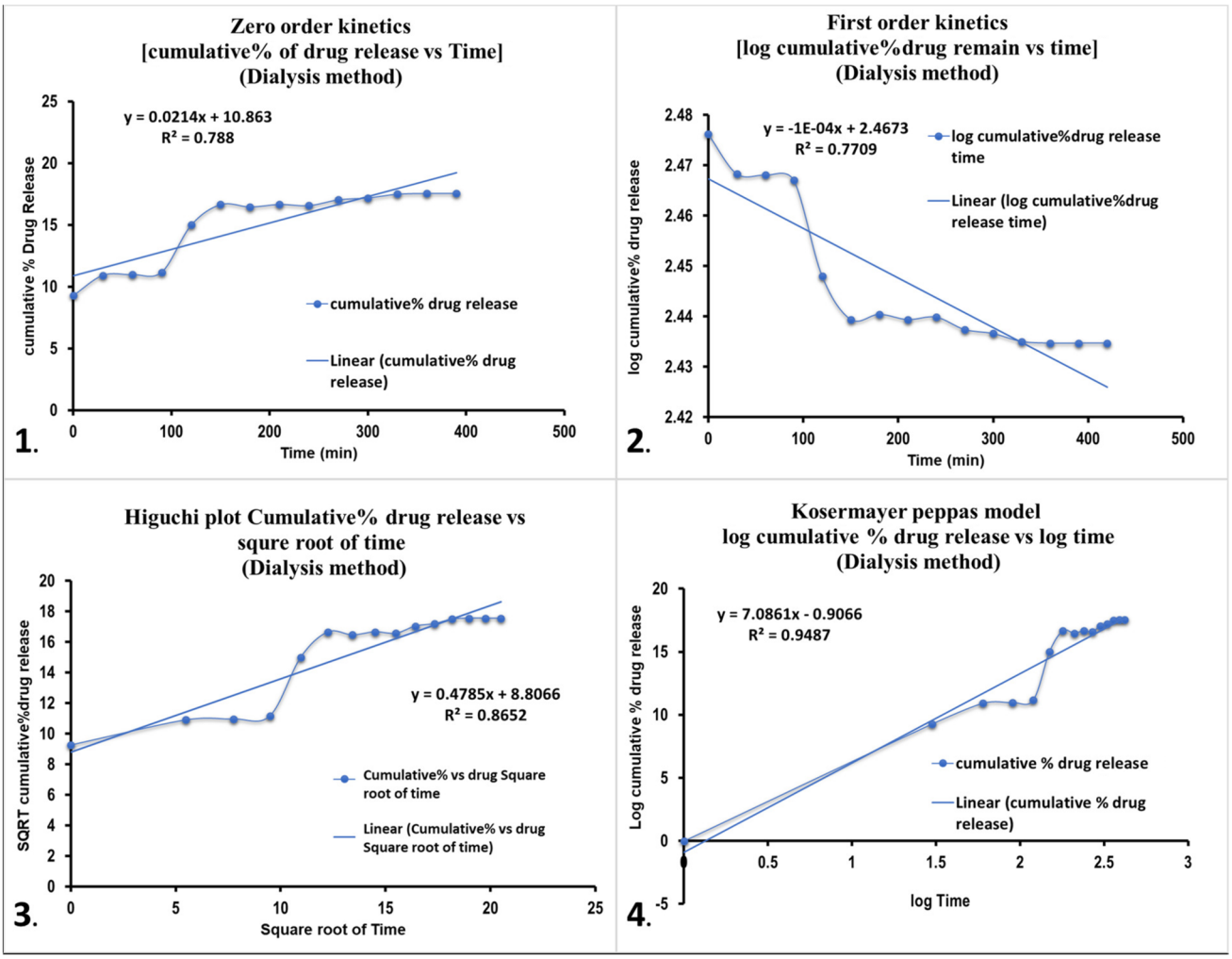

Fig. 10 Kinetics analysis of drug release by dialysis method: **1** zero-order kinetics, 2 first-order kinetics, **3** Higuchi plot, and **4** Kosermayer-Peppas model

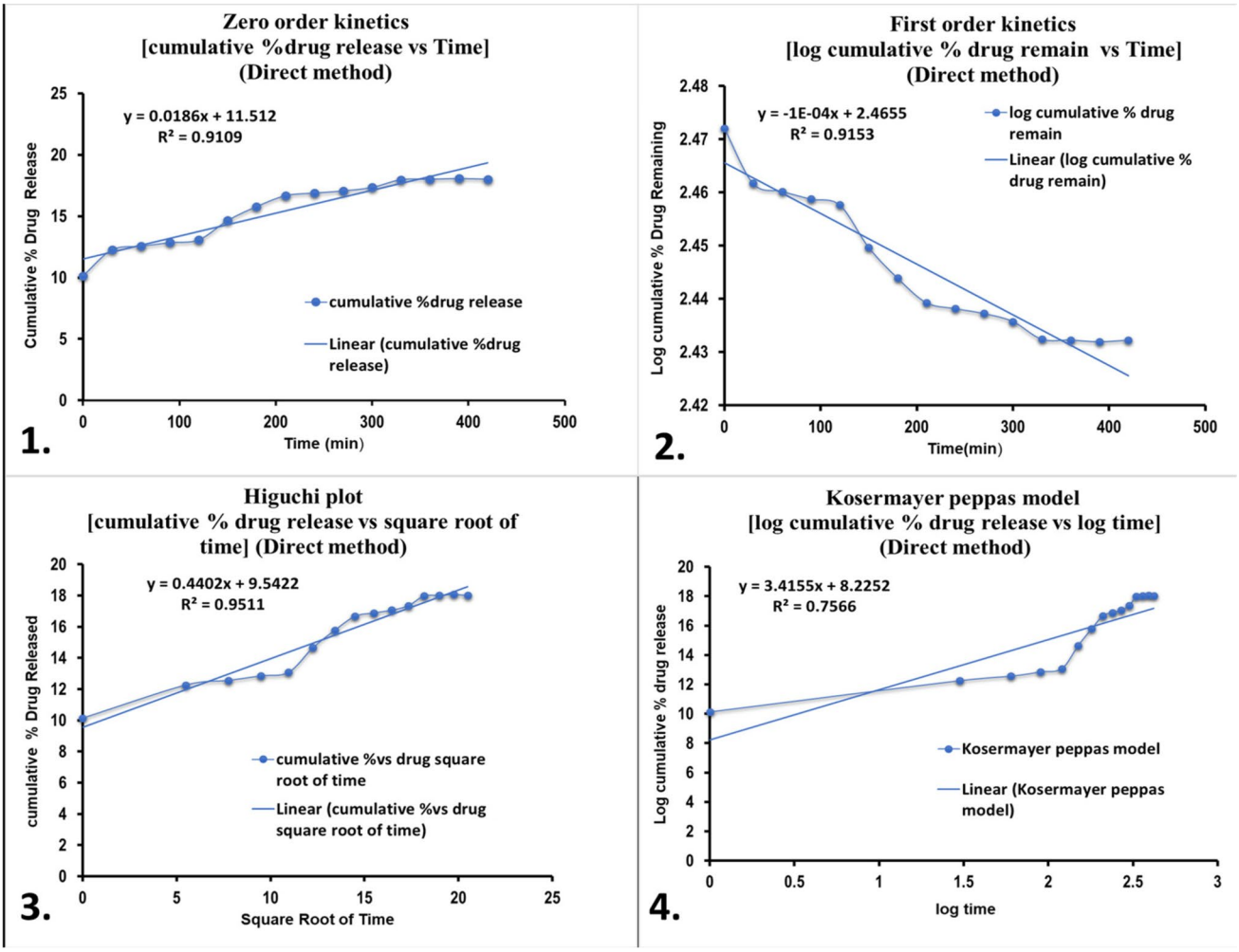

Fig. 11 Kinetics analysis of drug release by direct method: **1** zero-order kinetics, **2** first-order kinetics, **3** Higuchi plot, and (**4**) Kosermayer-Peppas model

the SPR of the nanocomposite, and the core optical properties as well as stability were determined. The nanocomposites showed a distinct antimicrobial activity with a display of antioxidant activity. With reference to the experimental data and the literature, it can be intrigued that the synthesized nanocomposite showed antibacterial activity against different microbes through the phenomenon of antioxidant activity which further causes imbalance in the physiology of the bacterial strains, thereby leading to the cell death of the microbes.

4 Future Prospects

Multidrug-resistant bacteria which is an ever-increasing problem these days could be resolved by using this biosynthesized eugenol-loaded nanocomposite. The major challenge is to discover the effective techniques for isolating and purifying newer and safer naturally occurring antimicrobials against MDR pathogenic microorganisms. A better understanding of the structure, function, and action mechanism of existing and newly identified antibiotics will help researchers to fine-tune proper design of the drug to work against MDR pathogenic microorganisms. The current research focuses on most common approach for antimicrobial therapy and checks on excessive use of antibiotics and the spread of antibiotic resistant bacteria. Furthermore, the basic technique for assessing antibiotic sensitivity is time consuming; thus, this therapy may help preventing unnecessary use of antibiotics and the spread of antibiotic resistance bacteria. The future of antibiotics requires advancement in the areas that are dependent on highly traditional methods. Thus, there is an urge to perform substantial changes in policy, an understanding of the mode of action of these drugs, and investment in alternatives to traditional antibiotics. The current study

may provide new insight in the development of accelerated wound healing phenomena/slows skin infection and allowing patients to take a more active role in daily wound/skin infection care while potentially lowering healthcare costs, in numerous forms such as bandages, antiseptics, or antiseptics which may be beneficial for patients to apply with ease and comfort.

5 Conclusion

The present work focuses on and highlights the biosynthesis of eugenol-loaded nanocomposite for enhancement of wound healing. Due to the existing major problems in wound healing, there is a need for easy, low costing, eco-friendly, and non-toxic biosynthesized nanocomposite for biomedical applications like wound healing. Eugenol was loaded successfully on the nanocomposite using the sonication technique. The loaded nanocomposite showed good antibacterial activity against wound-causing pathogens. Thus, a eugenol-loaded Ag-Ti-Co nanocomposite will be a promising alternative to develop an antibacterial agent against wound-causing microorganisms, which are multidrug-resistant strains of microbes. Accordingly, this research may accelerate wound healing by this biosynthesized Eu@NC.

Author Contribution Aarya Sahay: writing the manuscript. Rajesh Singh Tomar* contribute to the guidance and correction of the paper, Pallavi Singh Chauhan analyzed the results and designed the methodology of the research work, and Vikas Shrivastava was a role in improving the work. All authors read and approved the final manuscript.

Funding Self-funded/no external funding.

Data Availability Not applicable.

Declarations

Ethical Approval Not applicable.

Conflict of Interest The authors declare no competing interests.

References

1. Nasrollahzadeh, M., Sajadi, S. M., Sajjadi, M., & Issaabadi, Z. (2019). Applications of nanotechnology in daily life. In *Interface Science and Technology* (Vol. 28, pp. 113–143). https://doi.org/10.1016/B978-0-12-813586-0.00004-3
2. Patra, J. K., Das, G., Fraceto, L. F., Campos, E. V. R., Rodriguez-Torres, M. D. P., Acosta-Torres, L. S., … Shin, H. S. (2018). Nano based drug delivery systems: Recent developments and future prospects. *Journal of Nanobiotechnology 2018 16:1*, *16*(1), 1–33. https://doi.org/10.1186/S12951-018-0392-8
3. bhowmik, D., Kumar*, K. P. S., Yadav, A., Srivastava, S., Paswan, S., & Dutta, A. sankar. (2012). Recent trends in Indian traditional herbs Syzygium aromaticum and its health benefits. *Journal of Pharmacognosy and Phytochemistry*, *1*(1), 13–22.
4. Verma, S. K., Jha, E., Panda, P. K., Kumari, P., Pramanik, N., Kumari, S., & Thirumurugan, A. (2018). Molecular investigation to RNA and protein based interaction induced in vivo biocompatibility of phytofabricated AuNP with embryonic zebrafish. *Artificial Cells, Nanomedicine and Biotechnology, 46*(sup3), S671–S684. https://doi.org/10.1080/21691401.2018.1505746
5. Makkar, H., Verma, S. K., Panda, P. K., Pramanik, N., Jha, E., & Suar, M. (2018). Molecular insight to size and dose-dependent cellular toxicity exhibited by a green synthesized bioceramic nanohybrid with macrophages for dental applications. *Toxicology Research, 7*(5), 959–969. https://doi.org/10.1039/c8tx00112j
6. Barroso, A., Mestre, H., Ascenso, A., Simões, S., & Reis, C. (2020). Nanomaterials in wound healing: From material sciences to wound healing applications. *Nano Select, 1*(5), 443–460. https://doi.org/10.1002/NANO.202000055
7. Husain, S., Nandi, A., Simnani, F. Z., Saha, U., Ghosh, A., Sinha, A., … Verma, S. K. (2023). Emerging trends in advanced translational applications of silver nanoparticles: A progressing dawn of nanotechnology. *Journal of Functional Biomaterials*, *14*(1), 47. https://doi.org/10.3390/jfb14010047
8. Sarkar, B., Mahanty, A., Gupta, S. K., Choudhury, A. R., Daware, A., & Bhattacharjee, S. (2022). Nanotechnology: A next-generation tool for sustainable aquaculture. *Aquaculture*, *546*, 737330. https://doi.org/10.1016/J.AQUACULTURE.2021.737330
9. Guo, S., & DiPietro, L. A. (2010). Factors affecting wound healing. *Journal of Dental Research, 89*(3), 219. https://doi.org/10.1177/0022034509359125
10. Jiang, T., Li, Q., Qiu, J., Chen, J., Du, S., Xu, X., … Wu, Z. (2022). Nanobiotechnology: Applications in chronic wound healing. *International Journal of Nanomedicine*, *17*, 3125–3145. https://doi.org/10.2147/IJN.S372211
11. Ramos, A. P., Cruz, M. A. E., Tovani, C. B., & Ciancaglini, P. (2017). Biomedical applications of nanotechnology. *Biophysical Reviews 2017 9:2*, *9*(2), 79–89. https://doi.org/10.1007/S12551-016-0246-2
12. Khunkitti, W., Veerapan, P., & Hahnvajanawong, C. (2012). In vitro bioactivities of clove buds oil (Eugenia caryophyllata) and its effect on dermal fibroblast. *International Journal of Pharmacy and Pharmaceutical Sciences*, *4*(SUPPL.3), 556–560.
13. Cortés-Rojas, D. F., de Souza, C. R. F., & Oliveira, W. P. (2014). Clove (Syzygium aromaticum): A precious spice. *Asian Pacific Journal of Tropical Biomedicine, 4*(2), 90. https://doi.org/10.1016/S2221-1691(14)60215-X
14. Faiga, N. N., Rachmadi, P., & Meizarini, A. (2018). Neovascular pattern in wound healing after zinc oxide and curcuma longa rhizome extract dressing application. *Contemporary Clinical Dentistry, 9*(Suppl 2), S337. https://doi.org/10.4103/CCD.CCD_435_18
15. Sinha, A., Simnani, F. Z., Singh, D., Nandi, A., Choudhury, A., Patel, P., … Verma, S. K. (2022). The translational paradigm of nanobiomaterials: Biological chemistry to modern applications. *Materials Today Bio*, *17*. https://doi.org/10.1016/j.mtbio.2022.100463
16. Verma, S. K., Suar, M., & Mishra, Y. K. (2022). Editorial: Green perspective of nano-biotechnology: nanotoxicity horizon to biomedical applications. *Frontiers in Bioengineering and Biotechnology*, *10*. https://doi.org/10.3389/fbioe.2022.919226
17. Prabhu, P., Rao, M., Murugesan, G., Narasimhan, M. K., Varadavenkatesan, T., Vinayagam, R., … Selvaraj, R. (2022). Synthesis, characterization and anticancer activity of the green-synthesized hematite nanoparticles. *Environmental Research*, *214*. https://doi.org/10.1016/j.envres.2022.113864

18. Selvaraj, R., Pai, S., Vinayagam, R., Varadavenkatesan, T., Kumar, P. S., Duc, P. A., & Rangasamy, G. (2022). A recent update on green synthesized iron and iron oxide nanoparticles for environmental applications. *Chemosphere*, *308*. https://doi.org/10.1016/j.chemosphere.2022.136331
19. Vinayagam, R., Hebbar, A., Senthil Kumar, P., Rangasamy, G., Varadavenkatesan, T., Murugesan, G., … Selvaraj, R. (2023). Green synthesized cobalt oxide nanoparticles with photocatalytic activity towards dye removal. *Environmental Research*, *216*. https://doi.org/10.1016/j.envres.2022.114766
20. Vaseghi, Z., Tavakoli, O., & Nematollahzadeh, A. (2018). Rapid biosynthesis of novel Cu/Cr/Ni trimetallic oxide nanoparticles with antimicrobial activity. *Journal of Environmental Chemical Engineering, 6*(2), 1898–1911. https://doi.org/10.1016/J.JECE.2018.02.038
21. Alshameri, A. W., & Owais, M. (2022). Antibacterial and cytotoxic potency of the plant-mediated synthesis of metallic nanoparticles Ag NPs and ZnO NPs: A review. *OpenNano*, *8*, 100077. https://doi.org/10.1016/J.ONANO.2022.100077
22. Verma, S. K., Jha, E., Kiran, K. J., Bhat, S., Suar, M., & Mohanty, P. S. (2016). Synthesis and characterization of novel polymer-hybrid silver nanoparticles and its biomedical study. *Materials Today: Proceedings, 3*(6), 1949–1957. https://doi.org/10.1016/j.matpr.2016.04.096
23. Nisar, M. F., Khadim, M., Rafiq, M., Chen, J., Yang, Y., & Wan, C. C. (2021). Pharmacological properties and health benefits of eugenol: A comprehensive review. *Oxidative Medicine and Cellular Longevity*, *2021*. https://doi.org/10.1155/2021/2497354
24. Kumari, S., kumari, P., Panda, P. K., Pramanik, N., Verma, S. K., & Mallick, M. A. (2019). Molecular aspect of phytofabrication of gold nanoparticle from Andrographis peniculata photosystem II and their in vivo biological effect on embryonic zebrafish (Danio rerio). *Environmental Nanotechnology, Monitoring and Management*, *11*. https://doi.org/10.1016/j.enmm.2018.100201
25. Rahman, A., Chowdhury, M. A., & Hossain, N. (2022). Green synthesis of hybrid nanoparticles for biomedical applications: A review. *Applied Surface Science Advances*, *11*, 100296. https://doi.org/10.1016/J.APSADV.2022.100296
26. Chauhan, P. S., Shrivastava, V., & Tomar, R. S. (2018). Biofabrication of copper nanoparticles: A next-generation antibacterial agent against wound-associated pathogens. *Turkish Journal of Pharmaceutical Sciences, 15*(3), 238–247. https://doi.org/10.4274/tjps.52724
27. Khan, Z. (2020). Chitosan capped Au@Pd@Ag trimetallic nanoparticles: Synthesis, stability, capping action and adsorbing activities. *International Journal of Biological Macromolecules, 153*, 545–560. https://doi.org/10.1016/J.IJBIOMAC.2020.02.304
28. Sreedharan, S. M., & Singh, R. (2019). Ciprofloxacin functionalized biogenic gold nanoflowers as nanoantibiotics against pathogenic bacterial strains. *International Journal of Nanomedicine, 14*, 9905–9916. https://doi.org/10.2147/IJN.S224488
29. Kalam, M. A., Iqbal, M., Alshememry, A., Alkholief, M., & Alshamsan, A. (2022). Fabrication and characterization of tedizolid phosphate nanocrystals for topical ocular application: Improved solubilization and in vitro drug release. *Pharmaceutics, 14*(7), 1328. https://doi.org/10.3390/PHARMACEUTICS14071328/S1
30. Khalil, A. A., Rahman, U. U., Khan, M. R., Sahar, A., Mehmood, T., & Khan, M. (2017). Essential oil eugenol: Sources, extraction techniques and nutraceutical perspectives. *RSC Advances*. https://doi.org/10.1039/c7ra04803c
31. Nasrollahzadeh, M., Sajjadi, M., Iravani, S., & Varma, R. S. (2020). Trimetallic nanoparticles: Greener synthesis and their applications. *Nanomaterials, 10*(9), 1784. https://doi.org/10.3390/NANO10091784
32. Cahyono, B., A'Yun, Q., Suzery, M., & Hadiyanto. (2018). Characteristics of eugenol loaded chitosan-tripolyphosphate particles as affected by initial content of eugenol and their in-vitro release characteristic. *IOP Conference Series: Materials Science and Engineering*, *349*(1). https://doi.org/10.1088/1757-899X/349/1/012010
33. Muhammad, D. R. A., Tuenter, E., Patria, G. D., Foubert, K., Pieters, L., & Dewettinck, K. (2021). Phytochemical composition and antioxidant activity of Cinnamomum burmannii Blume extracts and their potential application in white chocolate. *Food Chemistry*, *340*, 127983. https://doi.org/10.1016/J.FOODCHEM.2020.127983
34. Hameed, M., Rasul, A., Waqas, M. K., Saadullah, M., Aslam, N., Abbas, G., … Shah, P. A. (2021). Formulation and evaluation of a clove oil-encapsulated nanofiber formulation for effective wound-healing. *Molecules*, *26*(9). https://doi.org/10.3390/MOLECULES26092491
35. Paswan, S. K., & Saini, T. R. (2021). Comparative evaluation of in vitro drug release methods employed for nanoparticle drug release studies. *Dissolution Technologies*, *28*(4), 30–38. https://doi.org/10.14227/DT280421P30
36. Chen, Z., Hu, Y., Li, J., Zhang, C., Gao, F., Ma, X., … Geng, F. (2019). A feasible biocompatible hydrogel film embedding Periplaneta. *International Journal of Pharmaceutics*, 118707. https://doi.org/10.1016/j.ijpharm.2019.118707
37. Loo, Y. Y., Rukayadi, Y., Nor-Khaizura, M. A. R., Kuan, C. H., Chieng, B. W., Nishibuchi, M., & Radu, S. (2018). In vitro antimicrobial activity of green synthesized silver nanoparticles against selected Gram-negative foodborne pathogens. *Frontiers in Microbiology*, *9*(JUL), 1–7. https://doi.org/10.3389/fmicb.2018.01555
38. Mohammed, A., Seid, M. E., Gebrecherkos, T., Tiruneh, M., & Moges, F. (2017). Bacterial isolates and their antimicrobial susceptibility patterns of wound infections among inpatients and outpatients attending the University of Gondar Referral Hospital, Northwest Ethiopia. *International Journal of Microbiology*, *2017*. https://doi.org/10.1155/2017/8953829
39. Hou, H., Mahdavi, B., Paydarfard, S., Zangeneh, M. M., Zangeneh, A., Sadeghian, N., … Sen, F. (2020). Novel green synthesis and antioxidant, cytotoxicity, antimicrobial, antidiabetic, anticholinergics, and wound healing properties of cobalt nanoparticles containing Ziziphora clinopodioides Lam leaves extract. *Scientific Reports*, *10*(1). https://doi.org/10.1038/S41598-020-68951-X
40. Chikezie, I. O. (2017). Determination of minimum inhibitory concentration (MIC) and minimum bactericidal concentration (MBC) using a novel dilution tube method. *African Journal of Microbiology Research, 11*(23), 977–980. https://doi.org/10.5897/ajmr2017.8545
41. Omara, S. T. (2017). MIC and MBC of honey and gold nanoparticles against methicillin-resistant (MRSA) and vancomycin-resistant (VRSA) coagulase-positive S. aureus isolated from contagious bovine clinical mastitis. *Journal of Genetic Engineering and Biotechnology*, *15*(1), 219–230. https://doi.org/10.1016/j.jgeb.2017.02.010
42. Woranuch, S., & Yoksan, R. (2013). Eugenol-loaded chitosan nanoparticles: I. Thermal stability improvement of eugenol through encapsulation. *Carbohydrate polymers*, *96*(2), 578–585. https://doi.org/10.1016/J.CARBPOL.2012.08.117
43. Soltanzadeh, M., Peighambardoust, S. H., Ghanbarzadeh, B., Mohammadi, M., & Lorenzo, J. M. (2021). Chitosan nanoparticles as a promising nanomaterial for encapsulation of pomegranate (Punica granatum l.) peel extract as a natural source of antioxidants. *Nanomaterials*, *11*(6). https://doi.org/10.3390/nano11061439
44. Bhakya, S., Muthukrishnan, S., Sukumaran, M., & Muthukumar, M. (2016). Biogenic synthesis of silver nanoparticles and their antioxidant and antibacterial activity. *Applied Nanoscience (Switzerland), 6*(5), 755–766. https://doi.org/10.1007/S13204-015-0473-Z/FIGURES/9

45. Sarteep, Z., Ebrahimian Pirbazari, A., & Aroon, M. A. (2016). Silver doped TiO2 nanoparticles: Preparation, characterization and efficient degradation of 2,4-dichlorophenol under visible light. *Journal of Water and Environmental Nanotechnology, 1*(2), 135–144. https://doi.org/10.7508/JWENT.2016.02.007
46. Mody, V. V., Siwale, R., Singh, A., & Mody, H. R. (2010). Introduction to metallic nanoparticles. *Journal of Pharmacy and Bioallied Sciences, 2*(4), 282. https://doi.org/10.4103/0975-7406.72127
47. Verma, S. K., Jha, E., Panda, P. K., Thirumurugan, A., & Suar, M. (2019). Biological effects of green-synthesized metal nanoparticles: A mechanistic view of antibacterial activity and cytotoxicity, 145–171. https://doi.org/10.1007/978-3-030-04477-0_6
48. Verma, S. K., Panda, P. K., Kumari, P., Patel, P., Arunima, A., Jha, E., … Suar, M. (2021). Determining factors for the nano-biocompatibility of cobalt oxide nanoparticles: Proximal discrepancy in intrinsic atomic interactions at differential vicinage. *Green Chemistry*, *23*(9), 3439–3458. https://doi.org/10.1039/d1gc00571e
49. Duque-Aristizábal, J. C., Isaza-Areiza, L. M., Tobón-Calle, D., & Londoño-Lopez, M. E. (2019). Antibacterial activity of silver nanoparticles immobilized in zinc oxide-eugenol cement against Enterococcus faecalis: An in vitro study TT - Actividad antibacteriana de nanopartículas de plata inmovilizadas en cemento de óxido de zinc-eugenol contra el. *Revista de la Facultad de Odontología Universidad de Antioquia, 30*(2), 154–165.
50. Husain, S., Verma, S. K., Yasin, D., Hemlata, A. Rizvi, M. M., & Fatma, T. (2021). Facile green bio-fabricated silver nanoparticles from Microchaete infer dose-dependent antioxidant and anti-proliferative activity to mediate cellular apoptosis. *Bioorganic Chemistry*, *107*. https://doi.org/10.1016/j.bioorg.2020.104535
51. Naser, D. K., Abbas, A. K., & Aadim, K. A. (2020). Zeta potential of Ag, Cu, ZnO, CdO and Sn nanoparticles prepared by pulse laser ablation in liquid environment. *Iraqi Journal of Science*, *61*(10), 2570–2581. https://doi.org/10.24996/ijs.2020.61.10.13
52. Zaichik, S., Steinbring, C., Jelkmann, M., & Bernkop-Schnürch, A. (2020). Zeta potential changing nanoemulsions: Impact of PEG-corona on phosphate cleavage. *International Journal of Pharmaceutics*, *581*(March), 119299. https://doi.org/10.1016/j.ijpharm.2020.119299
53. Kurpiers, M., Wolf, J. D., Steinbring, C., Zaichik, S., & Bernkop-Schnürch, A. (2020). Zeta potential changing nanoemulsions based on phosphate moiety cleavage of a PEGylated surfactant. *Journal of Molecular Liquids*, *316*, 113868. https://doi.org/10.1016/j.molliq.2020.113868
54. Loganathan, B., Chandraboss, V. L., Senthilvelan, S., & Karthikeyan, B. (2015). Surface enhanced vibrational spectroscopy and first-principles study of L-cysteine adsorption on noble trimetallic Au/Pt@Rh clusters. *Physical Chemistry Chemical Physics, 17*(33), 21268–21277. https://doi.org/10.1039/c4cp05170j
55. Jeyakumar, G. E., & Lawrence, R. (2021). Mechanisms of bactericidal action of eugenol against Escherichia coli. *Journal of Herbal Medicine*, *26*, 100406. https://doi.org/10.1016/j.hermed.2020.100406
56. Nandiyanto, A. B. D., Oktiani, R., & Ragadhita, R. (2019). How to read and interpret FTIR spectroscope of organic material. *Indonesian Journal of Science and Technology*, *4*(1), 97–118. https://doi.org/10.17509/ijost.v4i1.15806
57. Bedlovicová, Z., Strapác, I., Baláž, M., & Salayová, A. (2020). A brief overview on antioxidant activity. *Molecules*, 1–24.
58. Pohan, L. A. G., Kambiré, O., Nasir, M., & Ouattara, L. (2020). Photocatalytic and antimicrobial properties of [AgTiO 2]:[Clay] nanocomposite prepared with clay different ratios. *Modern Research in Catalysis, 09*(04), 47–61. https://doi.org/10.4236/MRC.2020.94004
59. Sardjono, S. A., & Puspitasari, P. (2020). Synthesis and characterization of cobalt oxide nanoparticles using sol-gel method Synthesis and Characterization of Cobalt Oxide Nanoparticles Using Sol-Gel Method, *040046*(April), 1–5.